

**Project Report
TIP-89**

**Integrated Propellant Storage
and Feed System:
FY18 Engineering Research
Technical Investment Program**

A. Steckel

09 May 2019

Lincoln Laboratory
MASSACHUSETTS INSTITUTE OF TECHNOLOGY
LEXINGTON, MASSACHUSETTS



This material is based upon work supported under Air Force Contract No. FA8721-05-C-0002
and/or FA8702-15-D-0001.

DISTRIBUTION STATEMENT A Approved for public release, distribution unlimited.

This report is the result of studies performed at Lincoln Laboratory, a federally funded research and development center operated by Massachusetts Institute of Technology. This material is based upon work supported under Air Force Contract No. FA8702-15-D-0001. Any opinions, findings, conclusions or recommendations expressed in this material are those of the author(s) and do not necessarily reflect the views of the U.S. Air Force.

© 2019 MASSACHUSETTS INSTITUTE OF TECHNOLOGY

Delivered to the U.S. Government with Unlimited Rights, as defined in DFARS Part 252.227-7013 or 7014 (Feb 2014). Notwithstanding any copyright notice, U.S. Government rights in this work are defined by DFARS 252.227-7013 or DFARS 252.227-7014 as detailed above. Use of this work other than as specifically authorized by the U.S. Government may violate any copyrights that exist in this work.

**Massachusetts Institute of Technology
Lincoln Laboratory**

**Integrated Propellant Storage and Feed System: FY18 Engineering
Research Technical Investment Program**

**A. Steckel
*Group 71***

Project Report TIP-89

09 May 2019

DISTRIBUTION STATEMENT A Approved for public release: distribution unlimited.

Lexington

Massachusetts

This page intentionally left blank.

ACKNOWLEDGEMENTS

MIT LL Collaborators

Finn O'Brien

Brian Savidge

Kyle Thompson

Harrison Delecki

Steve Gillmer

Mark Scanzillo

Derek Straub

Sean Crowley

Adam Shabshalowitz

Jesse Mills

Mark Padula

Bob Davis

This page intentionally left blank.

TABLE OF CONTENTS

Acknowledgements	iii
List of Figures	v
1. INTRODUCTION	1
1.1 Background	1
1.2 Summary of Fiscal Year 2017 Work	2
1.2.1 Surface Tension Tank Approach	2
1.2.2 PMD Hydrostatic Analysis	3
1.2.3 Determining the Contact Angle for 3D Printed Surface	4
1.2.4 Measurement of the Adhesion Tension	5
2. SELECTED PMD DESIGN	7
2.1.1 Bubble Rejection	7
2.1.2 PMD Deliverable Volume	7
2.1.3 Impact of Contact Angle on 3D Printed Surface	8
2.1.4 PMD Manufacturability: Aspect Ratio	11
2.1.5 Bubble Point	12
3. TANK DESIGN FOR METAL 3D PRINT	15
3.1 3D Printing Design Constraints	16
3.1.1 Internal Overhangs	16
3.1.2 Printing Orientation	16
3.2 Tank inspection	17
3.2.1 Powder Removal	18
3.3 Stress Analysis	19
3.3.1 Leak Detection	21
3.4 Proof Testing	22
4. SYSTEM DESIGN	25
4.1 System Design and Schematic	25
5. SUMMARY	27
6. REFERENCES	29

This page intentionally left blank.

LIST OF FIGURES

Figure No.		Page
1	block diagram illustrating integration of propulsion system with structure.	2
2	Why liquid acquisition devices (LAD) are required [2].	3
3	Hydrostatic balance of liquid surface in sponge PMD.	4
4	Contact angle.	5
5	Young's equation surface tension.	5
6	Bubble rejection.	7
7	PMD deliverable volume.	8
8	Impact of contact angle on deliverable volume.	9
9	PMD deliverable volume over different panels and thicknesses.	10
10	Selected PMD design with modified contact angle (lattice not pictured).	10
11	PMD aspect ratio.	11
12	Bending stress of thin plate.	12
13	"Center-Tube" of PMD and final PMD with lattice.	13
14	Porous barrier.	13
15	Integrated system schematic.	15
16	Printed tank.	16
17	Orientation on build plate.	17
18	Tank validation flow chart.	17
19	Powder removal with DI water setup.	18
20	Print anomaly.	19
21	Images of print anomaly in build video.	20
22	Leak check process.	22
23	Proof test summary.	23
24	Schematic.	26

This page intentionally left blank.

1. INTRODUCTION

This report relays the efforts conducted during FY18 to design a new type of cubesat propellant storage and feed system that could, if adopted for use by Laboratory programs, enable new types of missions. This system optimizes space for volume constrained cubesats and is intended for use on missions where there are no viable COTS propulsion solutions. The system is currently designed for use with H₂O₂ propellant, but could be used with many different types of liquid monopropellant.

1.1 BACKGROUND

A cubesat refers to a satellite made up of $10 \times 10 \times 10$ cm units (or a “U”). Cubesats have spiked in popularity with standardized launch and deployer options which leverage this fixed form factor. As a result, cubesats are primarily volume, rather than mass or power, constrained. New propulsion systems in development by academia and industry are 1U or larger, with the ability to stack units together to increase capacity. This approach will not work for all missions. For instance, on a 6U cubesat, working in units of 1U is 16% of the entire volume budget. This could result in large fractions of volume wasted. To maximize payload capacity, propulsion systems have to be custom designed to provide the exact amount of thrust necessary for the mission.

The image on the left of Figure 1 illustrates a volume allocation for a 3U cubesat. The dark blue represents a 1U propulsion system, this is modeled after the MS-130 system currently in development by Aerojet Rocketdyne. The other blocks represent different satellite subsystems, with the cyan color indicating the volume left for the payload. The right side indicates the propulsion system integrated with the spacecraft structure, which is intended to hold only enough fuel to perform necessary operations. Note that this illustration is not based on requirements for any kind of mission. The same subsystems are present, but the reduction in fuel volume and flexible form factor increase the space for the payload. The key to this technology is to design the propulsion system to have a flexible form factor and fit around the payload in unused volume areas. The intent is to let the payload be the driver for the cubesat’s layout.

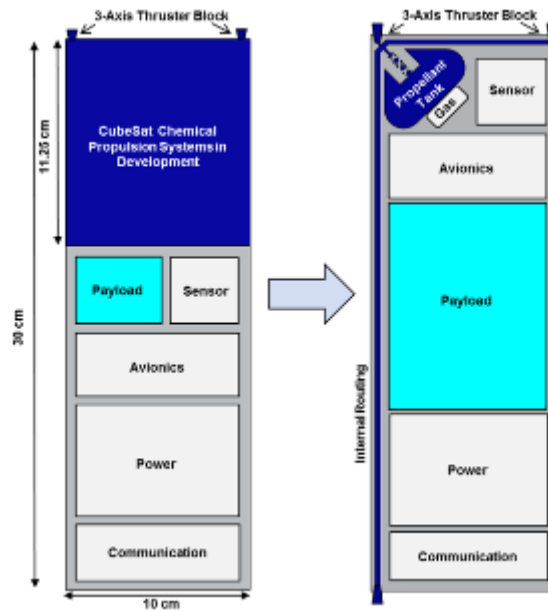


Figure 1: Block diagram illustrating integration of propulsion system with structure.

1.2 SUMMARY OF FISCAL YEAR 2017 WORK

1.2.1 Surface Tension Tank Approach

A surface tension tank is used to enable unconventional design form factors. In FY17, the focus was an analysis of the propellant management device (PMD, also called LAD), which is used in the propellant tank to control the location of the liquid in 0g. In this feed archetype, there is no barrier between the pressurant (gas) and the propellant (liquid) in the tank, as shown in Figure 2. The PMD ensures the system delivers only liquid fuel (with no gas bubbles) to the catalyst bed, thus ensuring predictable operation. PMDs are simple and require no moving parts, which make them ideal candidates for space systems. If required for the mission, PMDs can control the center of gravity of propellant. Surface tension tanks have flown on dozens of spacecraft missions [1], but none for cubesat fuel tanks at 10cm in diameter or smaller.

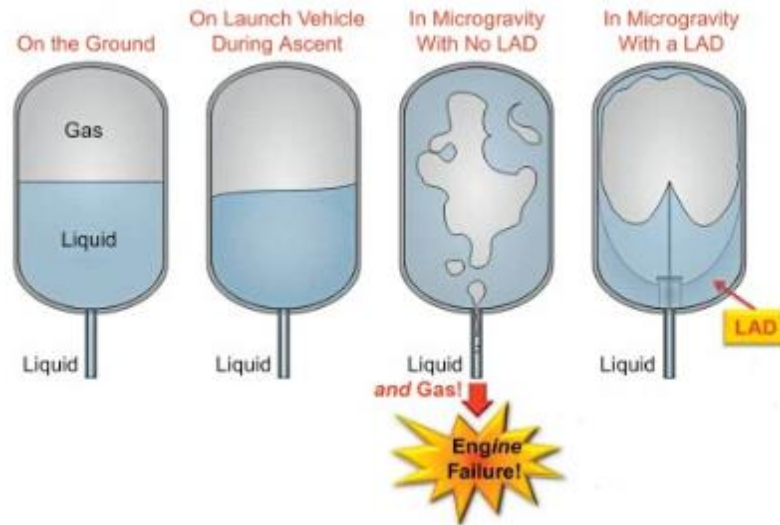


Figure 2: Why liquid acquisition devices (LAD) are required [2].

1.2.2 PMD Hydrostatic Analysis

A sponge style PMD, which traps liquid at the outlet of the tank, is selected for simplicity. A hydrostatic force balance on the PMD is used to develop an initial design, following the approach detailed in reference [3]. Equating the applied thrust with surface tension results in the following governing equation, Eq.1. [3]. Figure 3 shows the resulting shape of the liquid. This assumes flow loss from the PMD is negligible, and therefore does not apply while the thruster is firing. The solution of the governing equation forms the surface of the liquid, also shown in Figure 3 [3]. Any larger radius will drip out of the sponge and no longer be in control of the device. The computational model states that the radius selected must be smaller than the max radius before dripping. This determines the volume of available propellant in the PMD during operation.

$$\Delta P_{st} = \Delta P_{hy}$$

$$\sigma \left(\frac{1}{R_{up}} - \frac{1}{R_{low}} \right) = \frac{\rho a}{\sin\left(\frac{\pi}{N}\right)} (R_{up} + R_{low}) \quad 1$$

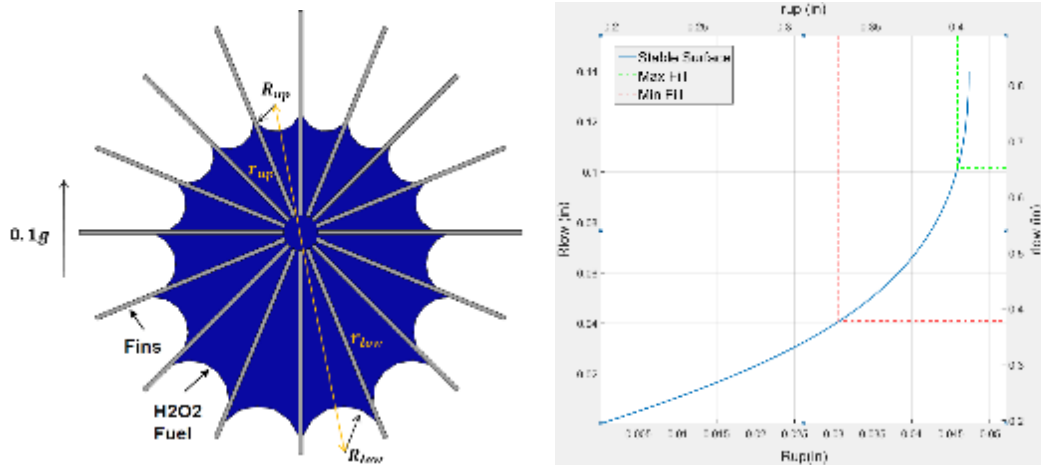


Figure 3: Hydrostatic balance of liquid surface in sponge PMD.

1.2.3 Determining the Contact Angle for 3D Printed Surface

A critical design parameter for these systems is the angle in which the fluid adheres to the walls of the PMD. This can loosely be compared to a material being hydrophobic or hydrophilic, where one surface has a greater ability to hold a liquid. Wenzel's equation states that rough surfaces enhance wettability [ref. 2, 3] is

$$\cos \theta_m = r \cos \theta_y$$

where,

θ_m measured contact angle

θ_y Young contact angle (ideal surface)

r roughness ratio.

The area factor, S_{dr} , relates roughness ratio to area factor: $r = 1 + S_{dr}/100$. S_{dr} and can be measured with a Taylor Hobson CCI White Light Interferometer. For this surface, it is on average 99.6%. This results in a contact angle of 52 degrees.

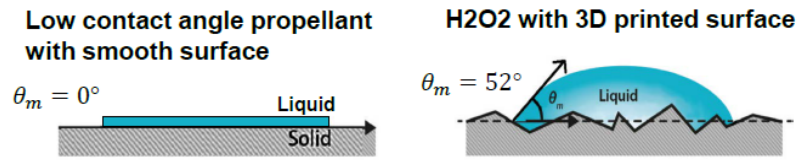


Figure 4: Contact angle.

1.2.4 Measurement of the Adhesion Tension

The contact angle is translated into an absorption measure with Young's equation defining surface tension [ref. 4],

$$\sigma_{sg} = \sigma_{sl} + \sigma_{lg} \cos \theta$$

Surface tension, σ_{lg} , is independent of the surface condition, however Adhesion tension ($A = \sigma_{sg} - \sigma_{sl}$) depends on roughness as defined by:

$$rA = \sigma_{lg} \cos \theta_m$$

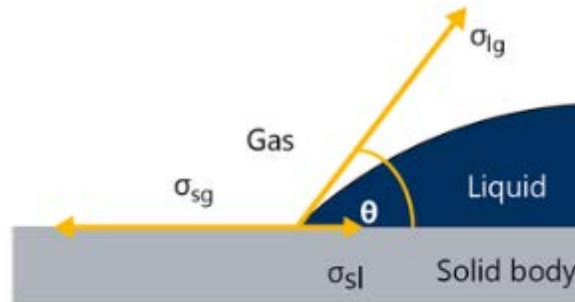


Figure 5: Young's equation surface tension.

These tension terms define how the H₂O₂ interacts with the PMD and the shape that droplets form on the surface. This angle of contact is a critical parameter to determining the amount of liquid adsorbed to the sponge. These principles were used in a computational model to design a ground test system.

This page intentionally left blank.

2. SELECTED PMD DESIGN

Continuing the analysis from the previous year, specific parameters of the design were determined during this fiscal cycle.

2.1.1 Bubble Rejection

Ultimately, the purpose of the PMD sponge is to ensure that bubbles do not enter the fuel nozzle plumbing. If a gas bubble could enter panels of the sponge, it can isolate propellant from outlet and cause a malfunction of the thruster. The taper inherent in the radial fins creates different radii on either end of the bubble. This difference in crosssectional area causes a force imbalance, which acts to push the bubble out of the PMD and into the greater tank volume. The minimum taper can be found by differentiating Young-Laplace equation.

$$\frac{dg}{dz} > \frac{\rho a g^2}{2\sigma \cos(\alpha)}$$

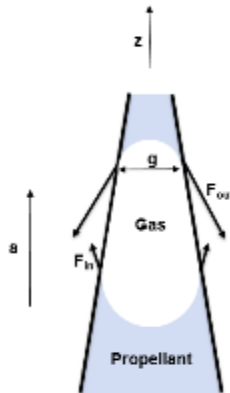


Figure 6: Bubble rejection.

2.1.2 PMD Deliverable Volume

The volume of gas-free propellant the sponge can deliver is calculated using Young-Laplace equation.

- Maximum Holding Volume: If more propellant is added, it will drip off
- Minimum Holding Volume: If more propellant is drained, gas may enter the thruster

Deliverable volume = Maximum Holding Volume – Minimum Holding Volume

For one design using 1" tall PMD and a 0° contact angle, the deliverable volume is 0.32 in³.

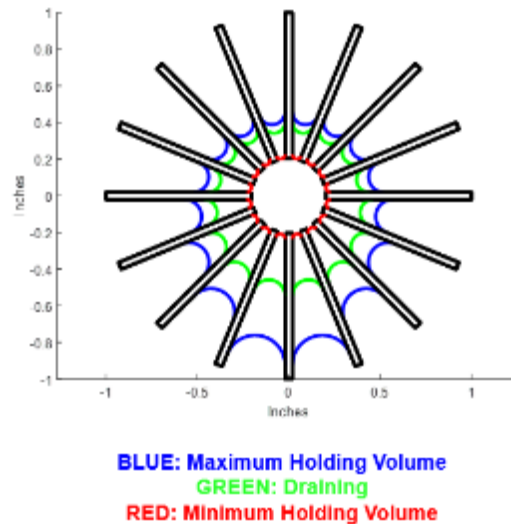


Figure 7: PMD deliverable volume.

2.1.3 Impact of Contact Angle on 3D Printed Surface

Modified Young's Equation is used to compute the contact angle for a rough 3D printed surface. Details are included in Section 1.2 of this report.

$$rA = \sigma_{lg} \cos \theta_m$$

3D printed material reduces the contact angle of the propellant in the sponge, which results in a smaller volume of propellant contained in the sponge. This analytical approach has been validated experimentally using a modified Wilhelmy-Plate method, as described in the FY 2017 technical report.

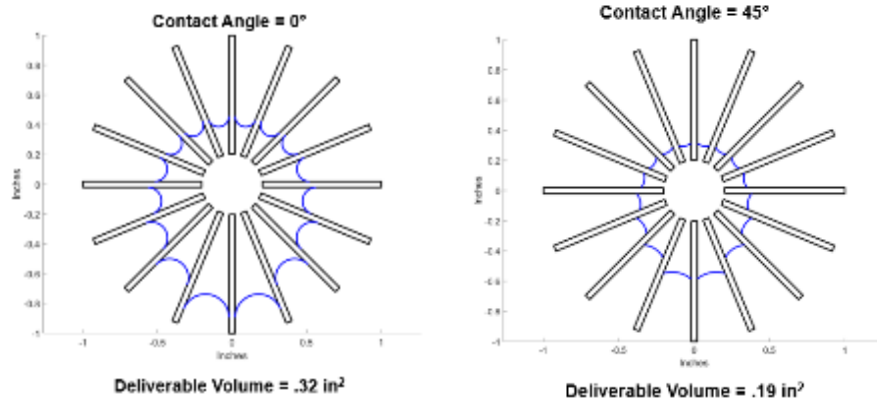


Figure 8: Impact of contact angle on deliverable volume.

Matlab is used to select an optimal PMD design. Figure 9 shows the solution to the governing equation (Eq. 1) over the indicated panel thicknesses and number of panels. The color bar indicates the volume in the PMD, and a value of -1 was used if the design did not meet the bubble rejection (Section 3.1.2) or manufacturability (3.1.1) criteria. This left a reduced phase space of available designs to down select from when considering tradeoff of manufacturability and effectiveness. The volume in the PMD is computed in Section 3.3.3.

The final design of the PMD is:

- Sponge radius of 1in
- 22 panels, .06 in thick
- 1 in tall
- Center tube filled with ~1 mm radius holes
- Deliverable volume: 0.21 in²
- Limiting acceleration for gas rejection: .12 g
- Bubble Point: 200 Pa

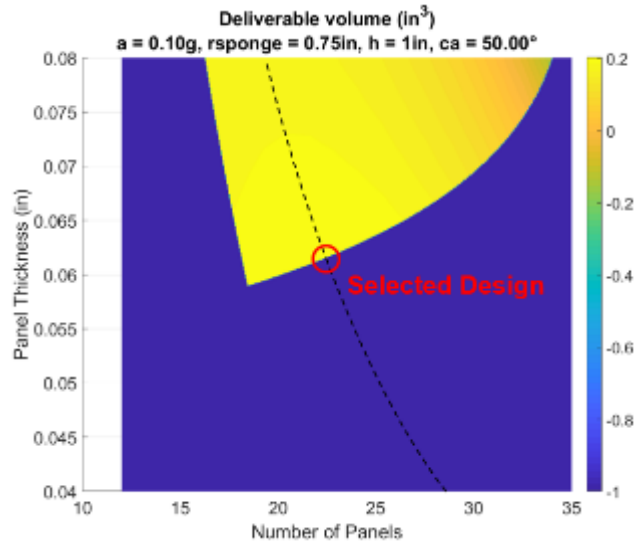


Figure 9: PMD Deliverable volume over different panels and thicknesses.

Below is a drawing of the final design with a minimum fluid surrounding the PDM whilst an acceleration is applied in the +y direction (in the plane of the page).

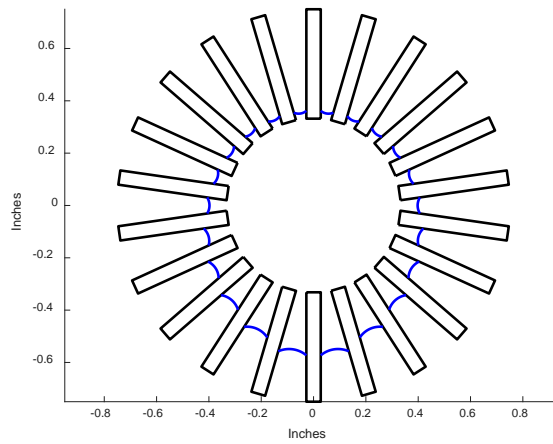


Figure 10: Selected PMD design with modified contact angle (lattice not pictured).

2.1.4 PMD Manufacturability: Aspect Ratio

Making the tank 3D printable constrains the design. To print the PMD, the tank has to be oriented as shown in Figure 11. It was determined that the fin aspect ratio (AR) is a critical parameter to produce a successful print. Once this constraint was discovered, 3D print iterations were conducted in house until the print failures disappeared. This occurred at an aspect ratio of 12.5. With a slight reduction in aspect ratio (11.25), the print was successful and was used as a minimal condition for the test tank. Results of these prints are shown in Figure 11.

$$AR = \frac{h}{t} = \frac{0.9''}{0.08''} = 11.25''$$

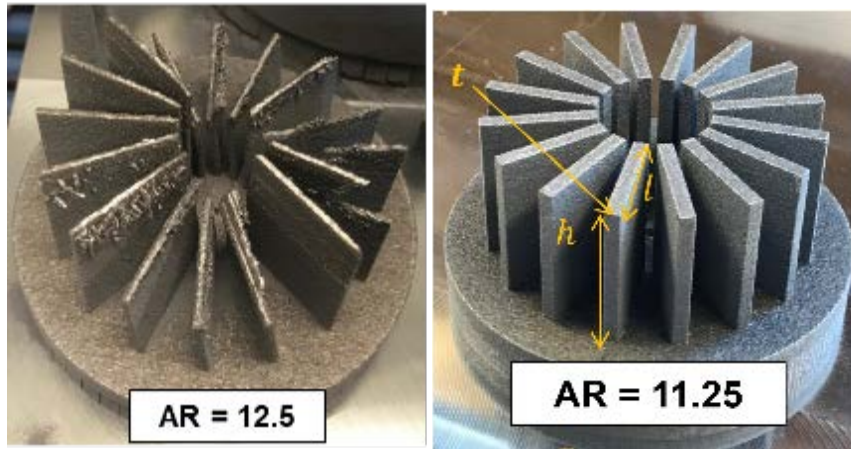


Figure 11: PMD Aspect Ratio

The printing failure was analytically modeled with the simple cantilever model shown below. These criteria can be used to evaluate manufacturability based on bending stress of a thin plate for future 3D printing works, shown in Figure 12.

$$\frac{\sigma_{max}}{F_{blade}} = \frac{6h}{It^2}$$

First print (failure):	$\frac{\sigma_{max}}{F_{blade}} = 3000 \text{ in}^{-2}$
Second print (success):	$\frac{\sigma_{max}}{F_{blade}} = 1205 \text{ in}^{-2}$

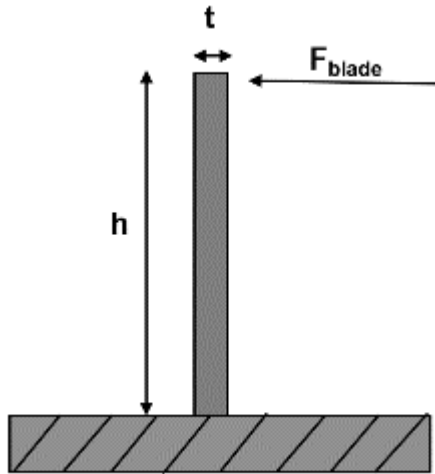


Figure 12: Bending stress of thin plate.

2.1.5 Bubble Point

The center tube (shown in Figure 13) of the PMD is too large to rely on surface tension or capillary action to prevent gas injection. This is due to the 0.04” gap between panels required to remove powder after printing. A porous device is added in center tube to block gas bubbles. The bubble point pressure (ΔP_{BP}) defines performance of a porous device. This is the minimum pressure required to prevent gas from flowing through the barrier. For this system, the bubble point is 200 Pa, which results in a maximum pore radius of 1mm. A lattice was added to the central tube with MAGICS software. A test print of the lattice was performed to verify a 1mm lattice is printable, which resulted in the successful print shown in Figure 13.

Derived from Young-Laplace Equation:

$$\Delta P_{BP} = \frac{2\sigma \cos(\alpha)}{r} = 200 \text{ Pa}$$

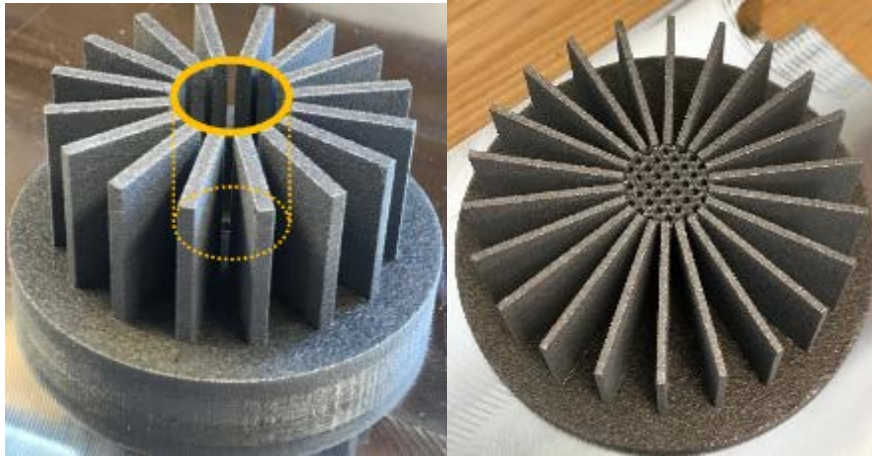


Figure 13: “Center Tube” of PMD and final PMD with lattice.

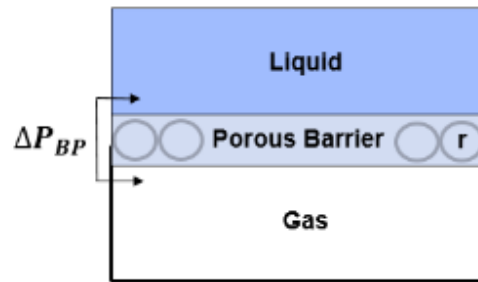


Figure 14: Porous barrier.

This page intentionally left blank.

3. TANK DESIGN FOR METAL 3D PRINT

Metal 3D printing is identified as a key technology to enable integration of the propulsion system with the satellite structure and fabrication of complex tank shapes. The pressurant and propellant tank are to be 3D printed and integrated together as shown in Figure 15 to optimize volume. 3D printing will simplify fabrication of future custom systems, making the propulsion system customizable and modular, as long as the design for metal 3D printing is well understood. For the flight system, a metal like Stainless Steel is compatible with H₂O₂ fuel. DMLS powder bed printers are industry standard for metal printing, and in these printers the design constraints are very similar with Stainless Steel or Aluminum powders. In-house capabilities of 3D printing aluminum were leveraged for this research.

Within the propellant tank, there is a fuel outlet, which has a firing valve and leads to the thruster manifold. The PMD is located at this outlet, which manages the location of the liquid and prevents gas bubbles from entering. In the propellant tank there is also a gas inlet for the pressurant. This region of the tank is designed to act as a diffuser, to slow the gas as much as possible. Reference Figure 15 for an illustration of the tank design and print direction.

The tank was fabricated in-house using the DMLS powder bed printer and AlSi10MG aluminum powder. The final printed tank is shown in Figure 16 before removal from the build plate.

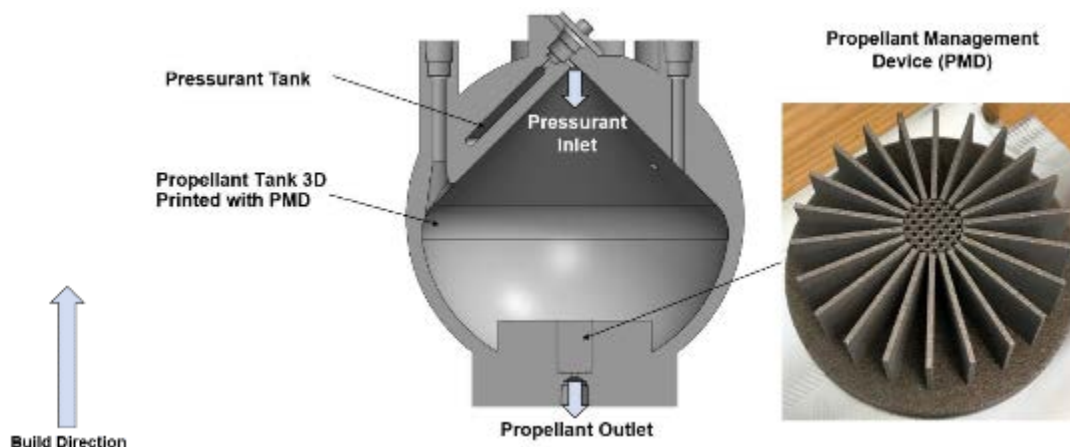


Figure 15: Integrated system schematic.



Figure 16: Printed tank.

3.1 3D PRINTING DESIGN CONSTRAINTS

3.1.1 Internal Overhangs

Internal overhangs must be 45° or steeper. If these overhangs are shallower, there is risk that the laser will melt more than one layer at a time, and there will be problems with the print. This gives the propellant tank a triangular shape on one end.

3.1.2 Printing Orientation

The orientation of the PMD (since it is a feature with a high aspect ratio) with respect to the cutting blade is also critical to manage during printing. It is important to avoid a 90° angle of the fins with respect to the cutting blade, as indicated by Figure 17.

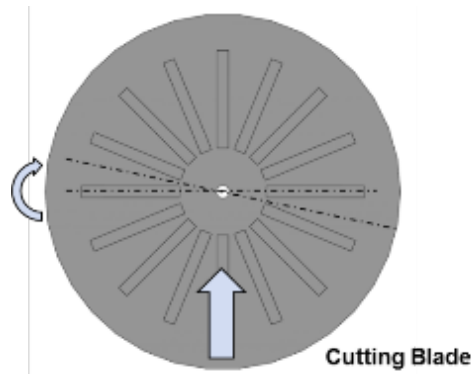


Figure 17: Orientation on build plate.

3.2 TANK INSPECTION

In order to remove powder after printing, each cavity must have at least 2 openings- one to insert gas to blow the powder out, and 1 exit for the powder. The flow chart shown below depicts the step by step process required to ensure that all debris is removed from the interior volume and ensure that the cavities are sealed.

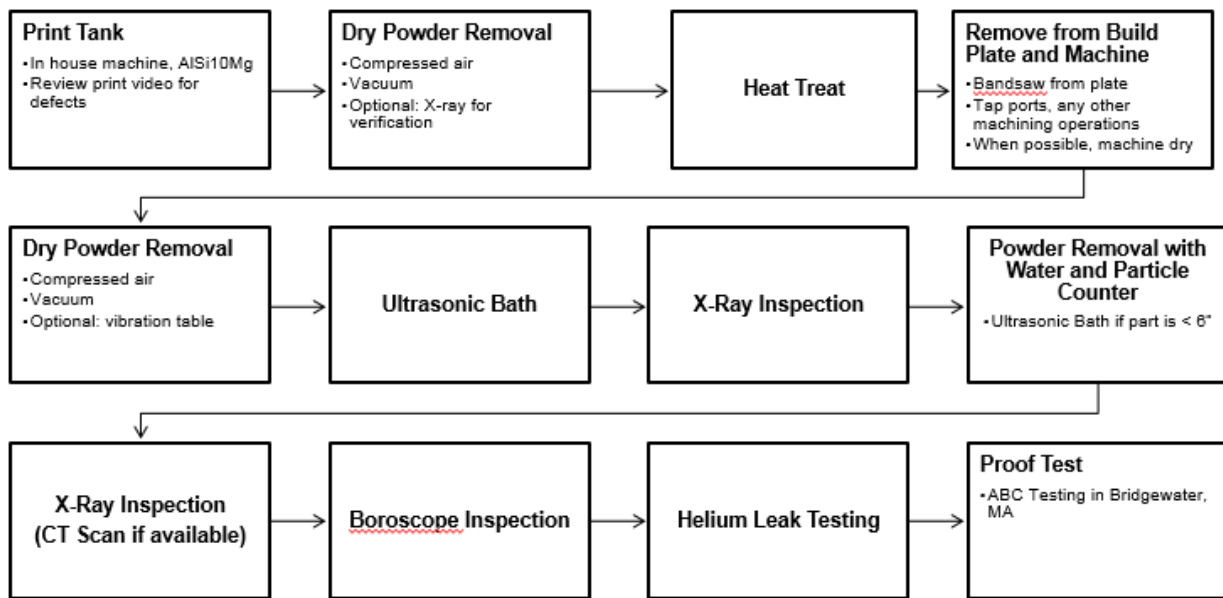


Figure 18: Tank validation flow chart.

Once the tank is printed, a gross cleaning occurs with pressurized gas and a vacuum. To ensure that the majority of the material has been removed various imaging techniques can be used. With the gross powder removed, the sintered material is heat treated to further solidify the walls. The part is removed from the build plate and cleaned once again with dry gas and a vacuum, before more powder is sonically dislodged. The final five stages of the flow chart verify that the tank produced is as designed.

3.2.1 Powder Removal

A “scoop” design has been incorporated to improve the flow of powder out of the chamber. These scoops required a detailed finite element analysis of the tank to consider high stress concentrations at these locations in the tank. In house processes were leveraged for additional powder removal. DI water was circulated through the tank to remove traces of powder. A particle counter measured particulate levels, and a filter removed particles as water circulated, as shown in Figure 19. This has the additional benefit of verifying the system won’t clog. The table below summarizes particle counts measured during this process, and in the final state.

Table 1: Particle Levels during DI Cleaning

Particle Size (um)	Particle Count at Start (/ml)	Particle Count at End (/ml)
> 25	>100	0
15-25	>100	<3
10-15	>1000	<10
5-10	>3000	<50

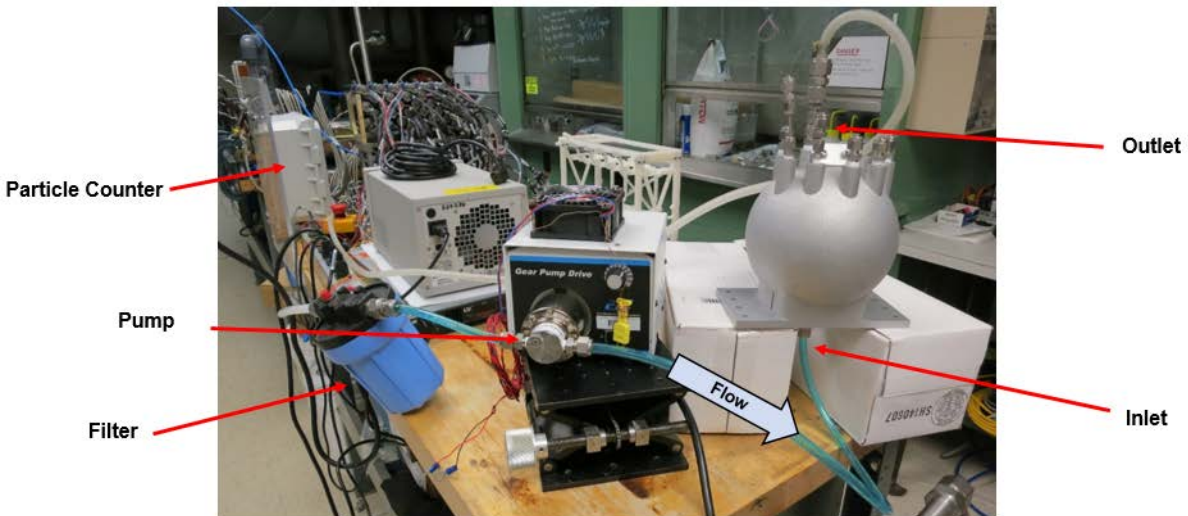


Figure 19: Powder removal with DI water setup.

3.3 STRESS ANALYSIS

The tank was originally designed to withstand 1,000 psi pressure on both tanks. However, some anomalies during print were identified during a boroscope inspection of the channels. A void which looks like a possible crack initiation site is photographed in Figure 20. This was located on the internal wall of the channel, and was not a threat to the outer walls of the tank. However, the boroscope is limited in with a short view distance, which means only the narrow channels and interfaces to the larger tanks can be inspected. This means there could be other voids printed in the larger chambers, where we cannot inspect. Funding for a CT scan (which has enough resolution to image these kinds of voids) was not originally budgeted, and was found to be prohibitively expensive. The tank was imaged with the in-house X-ray, and the build video was reviewed to attempt to identify other locations with anomalies. The anomaly was identified in the build video, as shown in Figure 21.

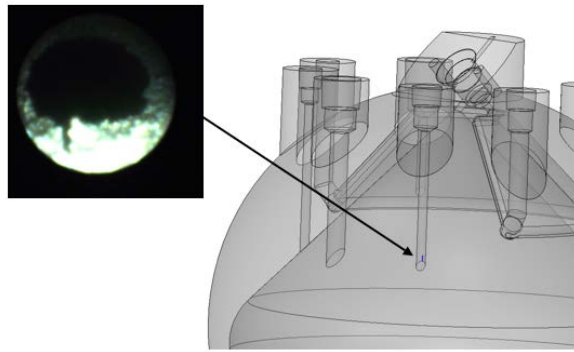


Figure 20: Print anomaly.

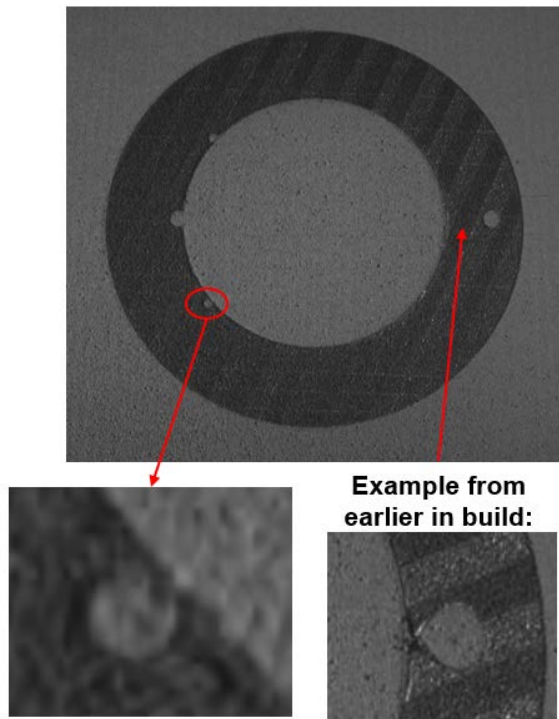
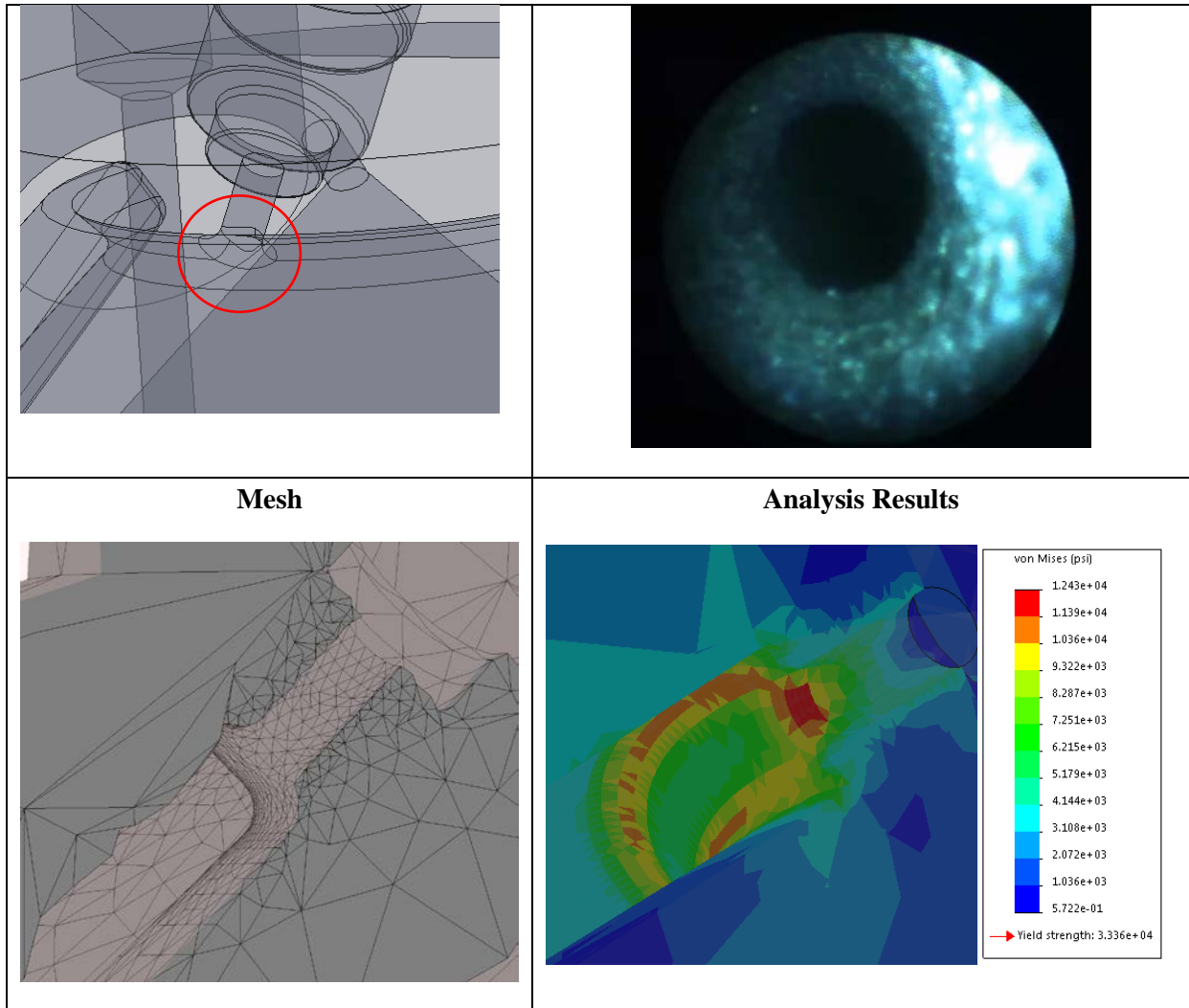


Figure 21: Images of print anomaly in build video.

A finite element analysis was performed on the system to verify the tank can safely handle pressure. Due to the unusual shape of the tank, there are several regions with high stress concentrations. Several iterations of the design were performed to reduce these stress concentrations and improve safety factor. The worst case stress concentration is shown below, located at the pressurant outlet of the tank. After printing, a boroscope of this region was performed to verify there were no printing anomalies prior to pressurizing.

<ul style="list-style-type: none"> • Highest Stress: 12.43 ksi • Safety Factor: 2.68 <p style="text-align: center;">Location on Tank</p>	<p>Boroscope Inspection</p>
---	------------------------------------



3.3.1 Leak Detection

The completed tank was checked for leaks with a standard helium 4 mass spectrometer. The leak rate from propellant tank and pressurant tank to atmosphere, as well as to one another were shown to have leak rates less than $5 \times 10^{-7} \text{ mbar L/s}$. A further test was done where the entire chamber was encased to determine if hairline cracks were present from the 3D printing process. Photographs of this process are shown in Figure 22.



Figure 22: Leak check process.

3.4 PROOF TESTING

The tank was proof tested at ABS testing in Bridgewater, MA. This was a hydrostatic test using water as the pressurant, because any failure would be safer than failing with gas pressurant. The tanks were tested to 1.3x Max Burst Disc Pressure, as defined Figure 23 below. This is more than 2x operating pressure. The tank was originally designed to hold 1,000 psi in all areas, which allowed for simplified analysis cases, and only ordering 1 kind of burst disc. However, after printing anomalies were identified in the propellant tank, this decision was revisited, since this tank will only be operating at 150 psig. New burst discs were ordered, and the pressures identified in orange were used for the proof test.

The proof test procedure is outlined below:

- Gradually increase to proof pressure up to 50% of max test pressure.
- Increase in 10% increments up to full test pressure.
- Hold for 15 min.
- Slowly remove pressure.

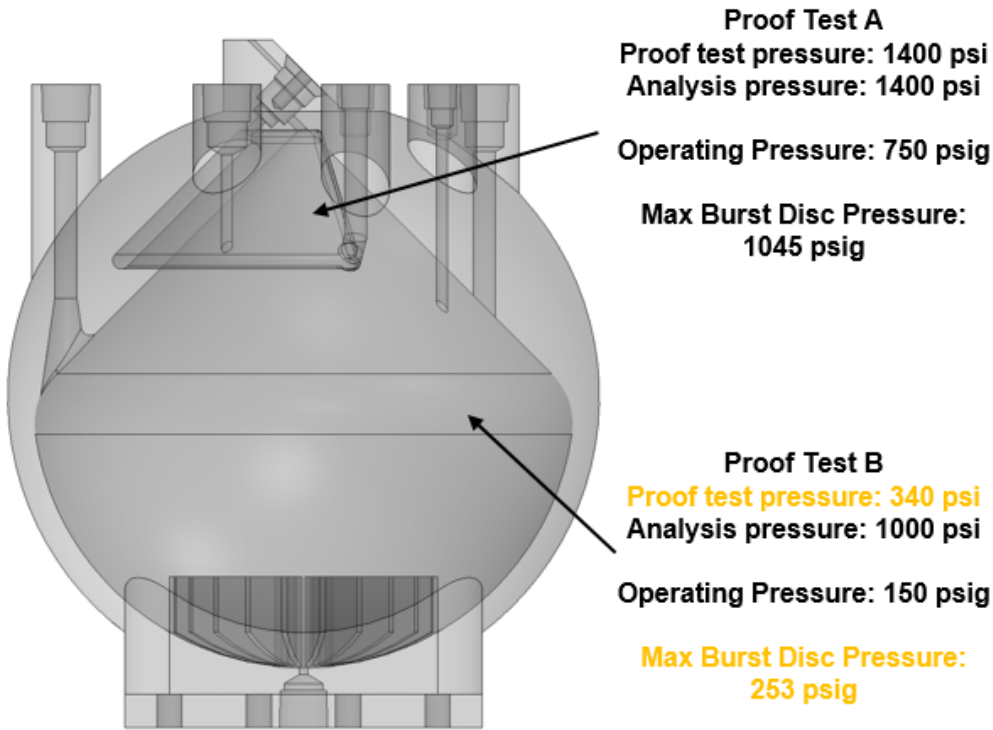


Figure 23: Proof test summary.

Results of the proof test were successful for the propellant chamber, which successfully held 340 psi for 15 min. The pressurant chamber reached 1400 psi, but steadily decreased to ~540 psi over a few minutes. There were no visible leaks during this test, and a post-test x-ray showed no deformation. After test completion, the regulator was removed and o-rings showed some damage. This indicates leaking through this seal to the other internal chamber.

To make the o-ring groove that seals between the two chambers, a custom cutter was ordered per the manufacturer's specifications. However, mechanical inspection found that even using this tool, the actual o-ring groove's OD was made .0056" larger than the maximum dimension called out on the print. Other dimensions of this groove, including the location and angle, were also out of tolerance per the print. This TI did not have funding to make a new tank or test this cutter out on other parts, but this is identified as the most likely cause of the leak at 1400 psi. Since the pressurant tank holds pressure at 540 psi, and since the volume of this tank was oversized, this should be sufficient to proceed with ground testing at MIT LL at the reduced maximum pressure of 540 psi.

This page intentionally left blank.

4. SYSTEM DESIGN

4.1 SYSTEM DESIGN AND SCHEMATIC

A ground test was designed and assembled to verify system requirements of delivering 0.4 LPM of propellant to the thruster. This system uses a positive expulsion tank to provide a regulated pressure to the thruster. The pressurant tank, green in Figure 24, is filled with pressurized nitrogen gas. This reservoir is kept separate from the propellant tank, blue in the same figure, by the passive pressure-regulating valve, valve 9. The pressurant tank will act as a ballast to maintain a constant pressure of 150 psi in the propellant tank. This design allows the propellant tank to be completely filled with liquid and the pressurant tank filled with compressed gas during launch, simplifying PMD requirements and slosh analysis. In addition to these two tanks and their operational connection, additional plumbing is required to ensure that the fill liquids are pure and without contamination, so the N₂ gas acts as a purge after testing. This will be required for future testing with H₂O₂, and is a good practice to avoid oxidation of the bare printed aluminum.

The valving system is designed to manage filling and pressurizing of the propellant and pressurant tanks. The process is initialized by opening 1, 2, 3, 6, and 7 to flow the respective fluids from their source and into the ambient environment. This will ensure that the fill lines coming from the liquid and gas source contain no contaminants for the later stages. Valve 6 and 3 will then be closed and valve 5 opened, to purge the liquid from the external plumbing system. After waiting sufficient time without observing any liquid emission from the port at valve 7, valve 5 can be shut and a nitrogen purge of the system will be conducted with the gas flowing from the N₂ source and through the storage tanks. This gas will be released to the ambient environment through valves 7 and 10. If desired, a pump phase can be implemented and alternated with the purge events by pumping on either of the two vent valves, 3 or 7. When the tanks are clean and full of nitrogen, the propellant tank will be evacuated through vent valve 7 before filling through the clean fill channels. When the tank is at pressure, valve 10 will be briefly opened to bleed propellant. At this point valve 3 can be shut and the pressurant tank filled in a comparable manner. With the tanks in this arrangement, tests can be conducted passively by closing valves 4 and 8 and controlling the flow with valve 10, or a combination of the nitrogen tank and vent valve 3 can be used to test the effects of different backing pressures on the output propellant flow. During operation, the manifold consisting of valves 1, 2, 3, 5, 6, and 7 can be removed.

The Premier Industries regulator valve, meets low SWaP requirements. Gas pressure must be above 150 psi, no higher than 750 psi, to work. The gas mass and volume are derived based on the requirement to blow out all propellant from the propellant tank, which is at 150 psi. For conservatism, and final pressure of 160 psi is used for the pressurant tank, so that it is always at a higher pressure than the propellant tank, and therefore able to expel all propellant.

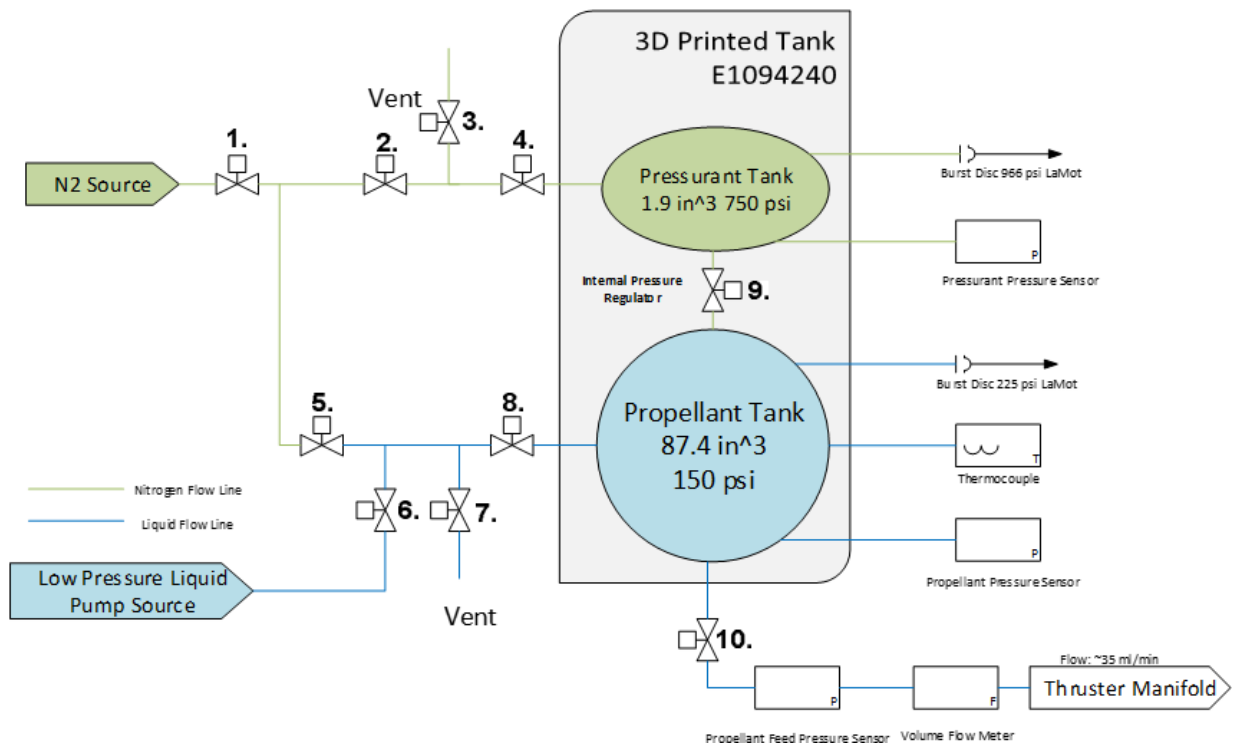
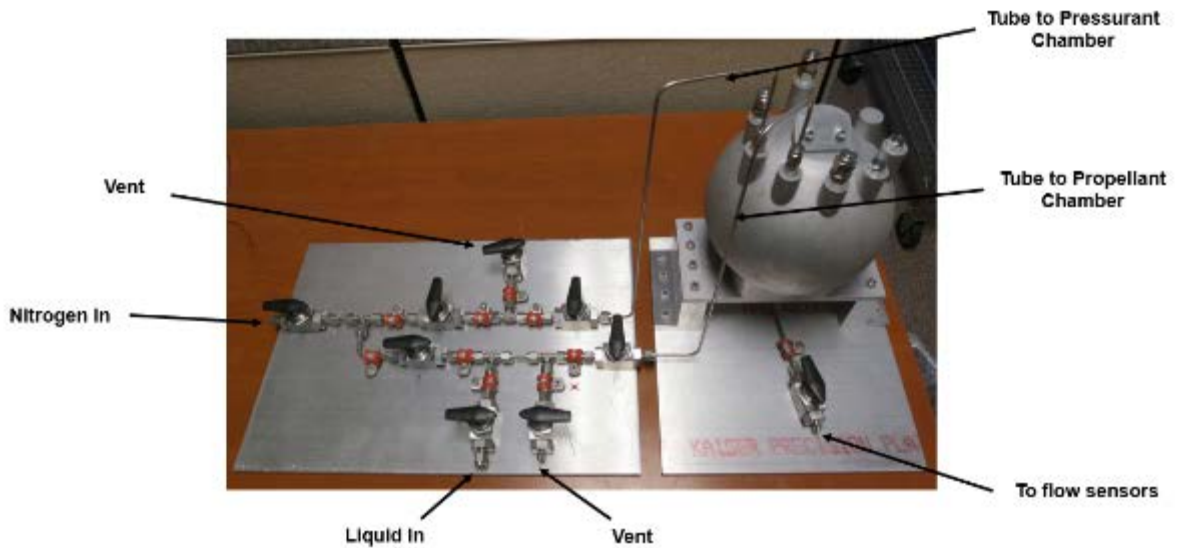


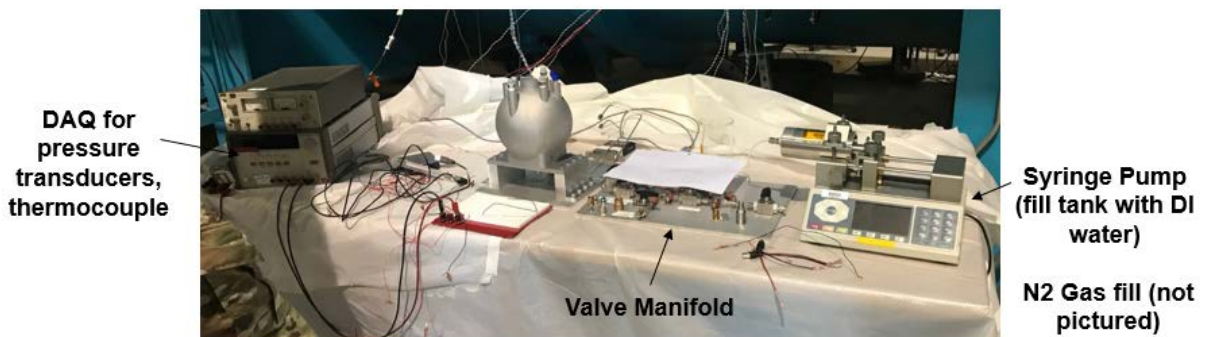
Figure 24: Schematic.

5. SUMMARY

The initial design for an integrated propellant storage and feed system has been developed. The propellant management device (PMD) drives the performance of the system. Based on the PMD analysis, a final design was selected. An integrated tank leveraging 3D printing was designed based on the requirements of the PMD. This tank was fabricated, and processes to remove powder, inspect printing flaws, and evaluate the sealing of the tank were implemented. The tank was proof tested at an external vendor, then attached to a manifold for use. A ground test of the system was designed to measure mass flow rate at the output of the tank, and to evaluate stability of the pressure at the outlet based on the passive pressure regulator expulsion method. Materials for the ground test have been procured and mostly assembled. At the time of this writing, the last status of test assembly is pictured below. Assembly work stopped when the co-op supporting the work reached the end of his term.



Flight Facility Test Setup 7/20/18



This research project is continuing during FY19, with a focus on maturing the PMD design and developing a flight system design. The impact of adhesion tension on the performance of the system will continue to be assessed in FY 19, and a conceptual 0g flight design will be matured to validate this work.

REFERENCES

- [1] J. R. Wertz and W. J. Larson, "Space Mission Analysis and Design," Third ed., Hawthorne, CA and New York, NY, Microcosm Press and Springer, 1999, pp. 708-716.
- [2] J. W. Hartwig, Liquid Acquisition Devices for Advanced In-Space Cryogenic Propulsion Systems, Academic Press, 2016.
- [3] J. D.E. Jaekle, "Propellant Management Device Conceptual Design and Analysis: Sponges," *AIAA 29th Joint Propulsion Conference and Exhibit*, 1993.
- [4] R. Wenzel, "Resistance of Solid Surfaces to Wetting by Water," *Industrial and Engineering Chemistry*, vol. 28, 1936.
- [5] "Young's Equation," 9 June 2017. [Online]. Available: www.kruss.de/services/education-theory/glossary/youngs-equation/.
- [6] Attention, "Influence of Surface Roughness on Contact Angle and Wettability," [Online]. Available: <http://www.dynetesting.com/>.
- [7] A. a. Y. Z. Faghri, Transport Phenomena in Multiphase Systems, Elsevier Academic Press, 2010.
- [8] D. Jaekle, "PMD Physics," 2011. [Online]. Available: www.pmdtechnology.com/PMD%20Physics.html.
- [9] S. W. Smith, "The Scientist and Engineer's Guide to Digital Signal Processing," [Online]. Available: <http://www.dspguide.com/pdfbook.htm>.
- [10] J. Bush, 18.357 *Interfacial Phenomena*, Massachusetts Institute of Technology: MIT OpenCourseWare, <https://ocw.mit.edu>. License: Creative Commons BY-NC-SA, Fall 2010, p. 9.
- [11] C. N. Satterfield, "Properties and Reactions of Hydrogen Peroxide," Massachusetts Institute of Technology Department of Chemical Engineering, Cambridge, Mass, 1962.

This page intentionally left blank.